














Obtaining a Zirconium dioxide-based photocatalyst using sol-gel method for turmeric degradation

Obtención de un fotocatalizador basado en dióxido de zirconio utilizando el método de sol-gel para la degradación de cúrcuma

Castrejón-Sánchez, Víctor Hugo^{*a}, Sánchez-Montiel, Dulce D.^b Enríquez-Pérez, Ma. Ángeles^c and García-González, Nidia^d

- ^a  TecNM: Tecnológico de Estudios Superiores de Jocotitlán •  C-9077-2015 •  0000-0002-0112-5388 •  235470
- ^b  Universidad Autónoma del Estado de México: Facultad de Química •  0009-0009-4298-1373 •  1316646
- ^c  TecNM: Tecnológico de Estudios Superiores de Jocotitlán •  H-9399-2018 •  0000-0002-2280-0661
- ^d  TecNM: Tecnológico de Estudios Superiores de Jocotitlán •  0000-0001-8968-1233 •  240047

CONAHCYT classification: DOI: <https://doi.org/10.35429/H.2024.12.67.83>

Area: Engineering
Field: Engineering
Discipline: Chemical Engineering
Subdiscipline: Materials Science


Key Handbooks

We explore the crystalline phase of ZrO2 obtained as a function of precursor molar ratios and the effectiveness of each crystalline phase in turmeric degradation. The key aspects are the crystalline phase transformations, the structural and morphological study of these phases and their application in photocatalysis. ZrO2 was synthesized by sol-gel, ammonia was used as catalyst, different phases were found as: monoclinic, tetragonal, cubic and a mixture of tetragonal with monoclinic; for different heat treatment temperatures; so the conditions for obtaining each of them could be determined. The behavior of the 4 samples obtained of ZrO2 as photocatalyst was evaluated. The phases that can degrade the organic pollutant turmeric are the tetragonal phase with a 24.98% degradation and the mixture of phases (tetragonal and monoclinic) with a 14.07% degradation.

Citation: Castrejón-Sánchez, Víctor Hugo, Sánchez-Montiel, Dulce, Enríquez-Pérez, Ma. Ángeles and García-González, Nidia. 2024. Obtaining a Zirconium dioxide-based photocatalyst using sol-gel method for turmeric degradation. 67-83. ECORFAN.

* ✉ [\[victor.castrejon@tesjo.edu.mx\]](mailto:victor.castrejon@tesjo.edu.mx)

Handbook shelf URL: <https://www.ecorfan.org/handbooks.php>



ISBN 978-607-8948-37-6/©2009 The Authors. Published by ECORFAN-Mexico, S.C. for its Holding Mexico on behalf of Handbook HCTI. This is an open access chapter under the CC BY-NC-ND license [<http://creativecommons.org/licenses/by-nc-nd/4.0/>]

Peer Review under the responsibility of the Scientific Committee MARVID®- in contribution to the scientific, technological and innovation Peer Review Process by training Human Resources for the continuity in the Critical Analysis of International Research.

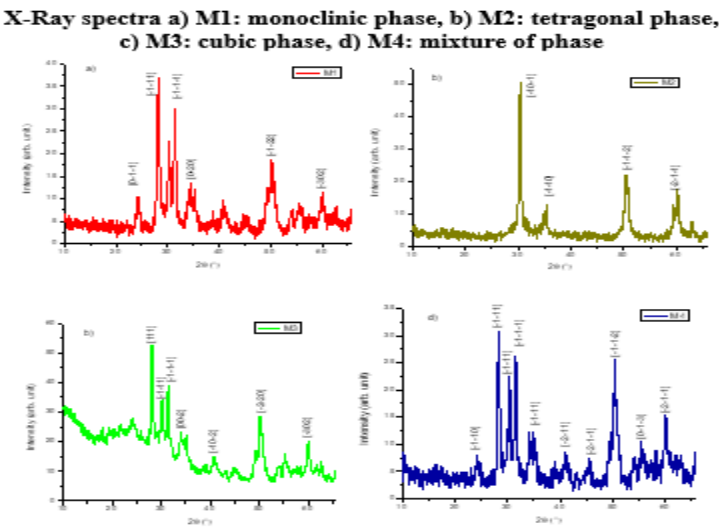


RENIECYT
Registro Nacional de Instituciones y
Empresas Científicas y Tecnológicas

1702902 CONAHCYT

Abstract

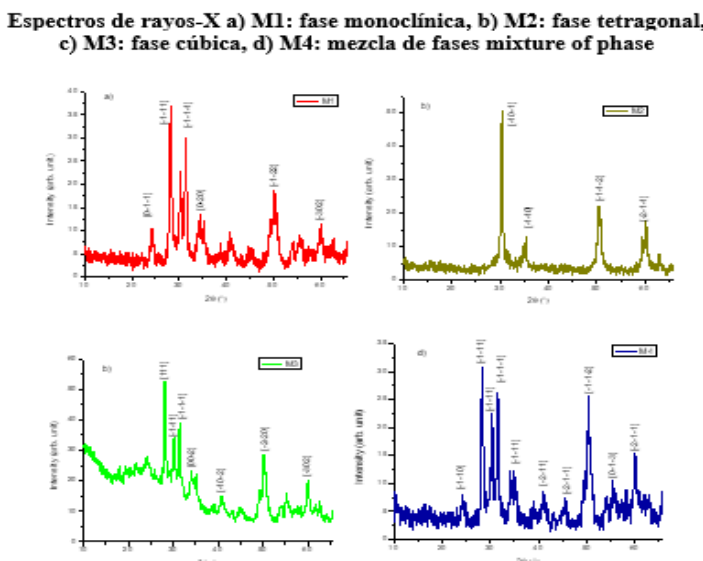
In this work, the synthesis, characterization, and evaluation of the photocatalytic properties of ZrO_2 are reported, which is used for the photocatalytic degradation of turmeric using UV light. The technique used for the preparation of zirconium dioxide is the sol-gel method. The samples were characterized using energy dispersive spectroscopy (EDS) to determine the chemical composition, and Scanning Electron Microscopy (SEM) was used to study the surface morphology. The chemical composition and crystalline phases present were analyzed with μ -Raman spectroscopy. The identification of crystalline planes was performed through X-Ray Diffraction. The synthesized ZrO_2 is composed solely of Zr and O, with no contaminants detected. No predominant type of morphology was found. Structural analyses revealed the phases present in each sample, which are: monoclinic, tetragonal, and a mixture of phases (monoclinic/tetragonal).



Zirconia, Crystalline phases, Turmeric degradation

Resumen

En este trabajo se reporta la síntesis, caracterización y evaluación de las propiedades fotocatalíticas del ZrO_2 , que se utiliza para la degradación fotocatalítica de la cúrcuma usando luz UV. La técnica empleada para la preparación del dióxido de circonio es el método sol-gel. Las muestras fueron caracterizadas utilizando espectroscopía de dispersión de energía (EDS) para determinar la composición química, y microscopía electrónica de barrido (SEM) para estudiar la morfología superficial. La composición química y las fases cristalinas presentes fueron analizadas mediante espectroscopía μ -Raman. La identificación de los planos cristalinos se realizó mediante difracción de rayos X. El ZrO_2 sintetizado está compuesto únicamente por Zr y O, sin que se detectaran contaminantes. No se encontró un tipo de morfología predominante. Los análisis estructurales revelaron las fases presentes en cada muestra, las cuales son: monoclinica, tetragonal y una mezcla de fases (monoclinica/tetragonal).



Zirconia, Fases cristalinas, Degradación de cúrcuma

Introduction

The increasing environmental pollution, as well as the accelerated consumption of fossil fuels, has caused a significant impact on nature, motivating the scientific community to develop clean energy sources as green chemical alternatives for water and air purification, water disinfection, hazardous waste remediation, and self-cleaning technology. In this context, heterogeneous photocatalysis has emerged as a "green" and environmentally friendly method that addresses these emerging issues. This process is characterized by a particulate photocatalyst suspended in a solution or in contact with a substrate in the gas phase and irradiated with sufficient energy to induce photoexcitation. Research on photocatalysis has increased exponentially since 1972, with the discovery of photo-assisted electrochemical water splitting using a TiO_2 single crystal as the working electrode and a platinum counter-electrode, under the application of a chemical or electrochemical potential (Nevárez-Martínez, Espinoza-Montero, Quiroz-Chávez, & Ohtani, 2017).

Zirconium oxide (ZrO_2)

Zirconium (IV) oxide, also known as zirconia, is a white crystalline oxide and a ceramic material. It belongs to the group of advanced ceramics, with properties such as high fracture resistance, toughness, hardness, elastic modulus, thermal expansion coefficient similar to metals, relatively high dielectric constant, low thermal conductivity, an energy gap of approximately 4.83 eV, and good corrosion resistance in both neutral and strongly acidic or alkaline environments (González, Flórez, Núñez, Chacón, & Sanz, 2012).

Zirconium oxide in its pure state does not exist in nature; it is found in the minerals baddeleyite and zircon. At ordinary temperatures, it has a very tightly packed hexagonal crystal structure and forms various compounds, such as zirconate or zirconyl salts. Zirconia is obtained in the form of a white powder and exhibits both acidic and basic properties (Deshmane & Adewuyi, 2012).

Uses

The applications of ZrO_2 are (Deshmane & Adewuyi, 2012) (Andrade-Guel, Cabello-Alvarado, & Ávila-Orta, Dióxido de zirconio: alternativas de síntesis y aplicaciones biomédicas, 2019):

- Thermal barrier coating
- Catalysis, for the removal of contaminants
- Electrode and oxygen sensors
- Orthopedic implants
- Useful as a coating for nuclear reactors
- Used as an additive in steels
- It is used for alloys with Nickel in the ceramic and glass industry.
- Useful for the manufacture of laboratory crucibles
- For coating ovens in the ceramic and glass industry
- It serves as a joint replacement because it is a bioinert material.

For the manufacture of vacuum tubes, heat exchangers and light bulb filaments

Crystalline phases

The chemical and physical properties of ZrO_2 depend on its crystalline structure; it is a polymorphic material, it has three crystalline phases (see figure 1), which are (Uuganbayar, Wen, & Y. Mostafa, Effect of Niobium on the Defect Chemistry and Oxidation Kinetics of Tetragonal ZrO_2 , 2014) (Thaleia V., 2009) (Beatriz, 2011):

1. Cubic: It is stable at a temperature between 2370 °C and the melting temperature (approximately 2680 °C). In its structure, each Zr^{4+} ion is coordinated with eight oxygen ions and in turn, each oxygen ion is tetrahedrally coordinated with four Zr^{4+} ions.
2. Tetragonal: It is stable at temperatures ranging between 1170 - 1200 °C to 2370 °C. It has a structure where each Zr^{4+} ion is surrounded by eight oxygen ions, four of them at a distance of 2.455 Å and the other four at a distance of 2064 Å. This phase is important because it provides greater tenacity and is the most stable phase.

3. **Monoclinic:** It is stable at temperatures below 1170-1200°C. In its structure, the Zr^{4+} cations are located in planes parallel to 001 and separated by the anion planes (O^{2-}). Each Zr^{4+} ion is surrounded by seven oxygen ions, such that it is triangularly coordinated with the oxygen ions of one OI plane, and tetrahedrally with the oxygen ions of a second OII plane. The thickness of the layers is greater when the Zr ions are separated by ions from the OI plane than when they are separated by oxygen ions from the OII plane.

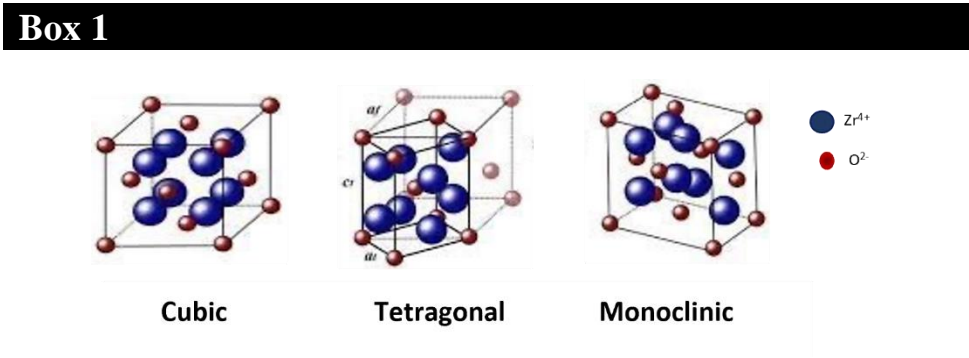


Figure 1
Crystalline phases of ZrO_2

Source: (Beatriz, 2011)

Sol-gel method

Concept

The sol-gel method is included within the soft chemistry methods for obtaining advanced high-tech inorganic materials, such as thin films, fibers, particles, etc. Because the method allows manipulation at the molecular level of the various stages of a Sol-gel reaction, it is possible to synthesize new high-purity materials by controlling the characteristics of the microstructure. The method also allows the control of surfaces and interfaces of the material during the last stages of the production process; for example, creating suitable compositional gradients on the surface (Gutierrez & Castellanos, 2021). In general, the process includes two main stages, which are: the dispersion of solid particles of colloidal size (1-100 nm) in a liquid phase and the gelation of the Sol; although other variants are also used such as (Gutierrez & Castellanos, 2021):

- a) hydrolysis and condensation of an alkoxide, or of the precursor nitrates, followed by hypercritical drying of the gel
- b) hydrolysis and polycondensation of the precursor alkoxides, followed by aging of the gel and drying under ambient conditions

1.1.1 Processing

It starts with a precursor, the sol formed by monomers in colloidal suspension. Alkoxides, which are also known as alcoholates, are commonly used precursors. They are compounds with the chemical formula $\text{M}(\text{OR})_2$ that are the result of the reaction between a metal M and an alcohol ROH (Pierre, 1998).

Secondly, the sol gradually evolves and forms a diphasic gel. The solid phase particles appear either discreetly or in the form of a polymer network. Third, the liquid part of the gel is removed. This can be done in several ways: sedimentation and centrifugation, among others (Pierre, 1998).

Afterwards, a drying and curing process is carried out. As the liquid evaporates, the substance shrinks and becomes denser. The evaporation rate of the solvent depends on the porosity of the gel. The microstructure of the final component depends on this stage of the process (see figure 2). Finally, the material is subjected to a thermal process that polycondenses the substance. This improves its mechanical properties and its structure, which becomes more stable (Bashir & Louise, 2015).

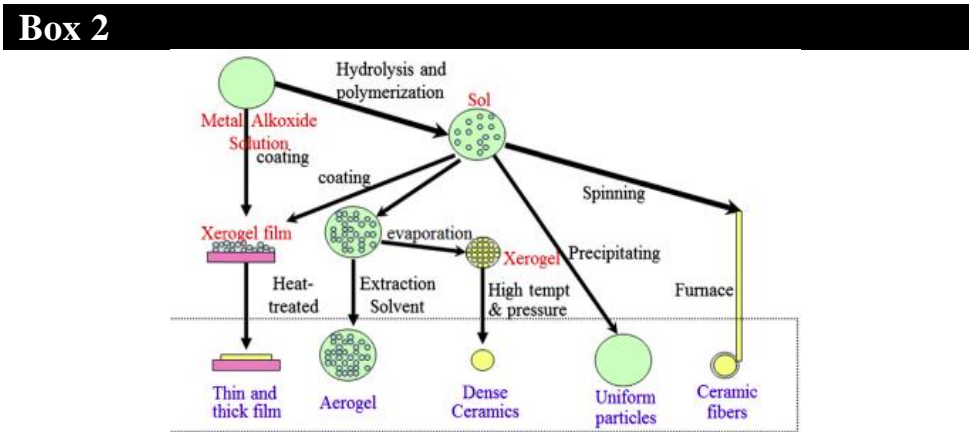


Figure 2
Sol-gel process

Source: (Bashir & Louise, 2015)

Applications

Some applications of the sol-gel process are described below (Bashir & Louise, 2015) (Ecológicos, 2024).

- **Protective coating:** The film formed by the sol-gel process can be deposited on the part by dipping or spraying. Coatings can be applied to glass, ceramics and other substrates, sometimes for decorative purposes.
- **Insulators:** Ceramic fibers with refractive properties can be obtained. For example, to manufacture thermal insulators.
- **Nano and microspheres:** Uniform ultra-fine grain ceramic powders can be obtained. These nanoparticles are useful, for example, in dental and biomedical applications. Chemical phytosanitary products such as herbicides have also been used successfully.
- **Medicine:** As a wound healer and stabilizer; also, to regulate the uniform and progressive release of active ingredients.

Table 1 shows an analysis of the sol-gel method applied for obtaining different material.

Box 3

Table 1		
Research articles related to materials obtained by sol-gel method		
Article title	Author	Results
Síntesis de TiO ₂ , fase anatasa, por el método sol-gel: estudio del efecto de la presencia de AcacH en el sistema.	(Ochoa, Ortegón, & Páez, 2010)	Obtaining submicrometric TiO ₂ particles, well-crystallized anatase phase.
Síntesis por Sol-gel de un recubrimiento nanoestructurado de TiO ₂ para ser aplicado en sustrato de vidrio.	(Ramírez-Riaño, 2017)	Precursor: titanium tetraisopropoxide and hydrogen peroxide. It made was possible to establish the best conditions for obtaining hydrophobic coatings.
Síntesis y Caracterización de Nanopartículas de Dióxido de Titanio Obtenidas por el Método de Sol-Gel	(Mosquera, N. Rosas, & Guerrero, 2015)	Precursor: titanium oxysulfate. The best synthesis conditions include calcination at 500 °C for 1 hour, which obtained particles smaller than 10 nm.
Síntesis y caracterización de materiales nanoestructurados de TiO ₂ por el método de sol-gel.	(Castrejón-Sánchez, Enríquez-Pérez, Rosales-Davalos, & Díaz-Camacho., 2018)	Obtaining titanium dioxide nanoparticles with different phases as well as structural, compositional and morphological characterization.
Estudio de los Procesos Sol-gel para la Obtención de un Aglutinante Apropriado para el Peletizado de Alúmina	(Carballo-S. & Galindo-V., 2011)	Results obtained in the tests and experimental exploration of an alumina forming technique are presented. Sol-gel processes are used in the production of a suitable binder for γ-Al ₂ O ₃ .
Preparación de SiO ₂ por los métodos no hidrotérmico y Sol-Gel para adsorción de colorantes	(Sánchez, Esteban, Ceja, & Altillano, 201731-36)	Preparation of mesoporous silicates was carried out by the Sol-Gel and non-hydrothermal method, with the purpose of comparing the textural and morphological properties of the resulting materials to be used in dye adsorption tests.

Photocatalysis

Concept

Photocatalytic activity is the property of a solid material induced by the irradiation of photons with energy equal to or greater than the energy of the bandgap of the material on its surface, which causes the e^- of the valence band to be excited towards the driving band and leave gaps in the first band. In this way, e^- - h^+ pairs called excitons are generated, they can be used to carry out redox reactions. Photocatalysis is the union of photochemistry and catalysis. Together, the light and the catalyst will slow or accelerate a chemical reaction, it can be thought of as the acceleration of a photoreaction through a catalyst (López, 2015) (Roberto J. Candal, s.f.).

Photocatalysis can be classified as a principle of decontamination of nature itself. Just as photosynthesis, through sunlight, can eliminate CO_2 by generating organic matter, photocatalysis is responsible for eliminating another type of pollutant that is also common in the atmosphere through the oxidation process that is caused using solar energy. With photocatalysis, solar energy is converted into chemical energy. To achieve this type of energy, a catalyst or substrate is needed. It must be a semiconductor material to accelerate the reaction rate. This process is used to reduce contaminants, where oxidation and reduction reactions take place (López, 2015) (Roberto J. Candal, s.f.).

Types of photocatalysis

Heterogeneous photocatalysis

It is generated from the illumination of a semiconductor catalyst with a photon. The photon must have an energy $h\nu$, equal to or greater than the value of the bandgap energy (E_g) of the photocatalyst for an electron from its valence band to be promoted to the conduction band (Nevárez-Martínez, Espinoza-Montero, Quiroz-Chávez, & Ohtani, 2017).

The bandgap energy is the energy difference between the valence band and the conduction band of the photocatalyst. This fact leads to the formation of two charge carriers: electrons in the conduction band, and a positive empty electron in the valence band known as a “hole” (see figure 3). That is, when an electron leaves the valence shell and becomes a free electron, a “hole” is created. This phenomenon is known as an electron-hole pair. Electrons in the excited state within the conduction band and holes within the valence band can recombine to the initial state and dissipate the obtained energy as heat. But they can also be trapped in metastable surface states or react with molecules adsorbed on the semiconductor surface, accepting and donating electrons (Nevárez-Martínez, Espinoza-Montero, Quiroz-Chávez, & Ohtani, 2017).

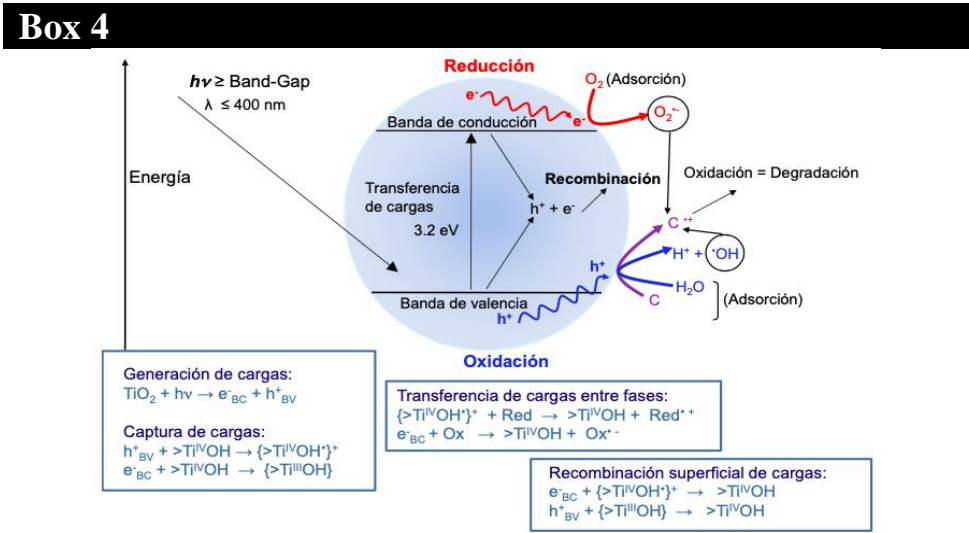


Figure 3
Schematic representation of a photocatalytic process on a semiconductor particle

Source: (Zarazúa-Acosta, 2023)

1.4.2.2 Homogeneous photocatalysis

In homogeneous phase photocatalytic processes, the capacity to absorb photons is established, so the contaminant and light can also lead to the chemical modification of the substrate. The process of homogeneous photocatalysis arises when it is demonstrated that hydrogen peroxide could be activated by salts to oxidize tartaric acid and subsequently is called “free radical pathways” (Zarazúa-Acosta, 2023).

1.4.3 Components necessary for photocatalytic process

For the photocatalytic reaction to be carried out, the following are needed: compound and/or substance to be degraded, oxidant such as oxygen contained in air, a medium where the reaction takes place, such as air, a photocatalyst, usually a semiconductor compound, broadband, and a visible or ultraviolet light source, whether natural or artificial (Zarazúa-Acosta, 2023).

1.4.3.1 Photocatalyst

It is a semiconductor material that accelerates the speed of the oxidation reactions that take place on its surface, through its excitation with light with a photon energy equal to or greater than its E_g . The semiconductor material must meet a series of requirements to be an effective photocatalyst, such as (LODEPA, 2023):

- Chemical inertness and molecular stability in contact with water, that is, resistance to photo-corrosion and insolubility.
- Redox potential of the conduction band positive enough to oxidize the hydroxyls and in the case of the valence band, negative enough to reduce oxygen or the species to be reduced.
- Bandgap that allows it to be activated by sunlight.
- Low toxicity since the aim is to reduce contaminating compounds.
- Availability at reduced cost.

Oxidant

Oxygen is an element that can oxidize a photocatalyst and accept electrons; although there are also metallic cations that can play this role. In the gaseous phase, it is easy to provide oxygen, since it is found in abundance in the air (Nevárez-Martínez, Espinoza-Montero, Quiroz-Chávez, & Ohtani, 2017) (Fujishima, Zhang, & Tyrk, 2008).

Electron supply

The compounds that provide electrons to the process are usually from the OH^- group and react to form the hydroxyl radical that subsequently favors the oxidation of adsorbed species. Although it is worth mentioning that it has been proven that, in the gaseous phase where there is no water saturation, there are other adsorbed molecules that act as electron donors by oxidizing directly (Fujishima, Zhang, & Tyrk, 2008).

Ultraviolet Light (UV)

Photocatalysis can occur under the influence of sunlight and artificial light. The latter has the advantage that it can be used with only one UV wavelength, choosing the one that excites the semiconductor to begin its work (Lisbona-García, 2016).

1.5 Organic Pollutants

Persistent Organic Pollutants (POPs) are a group of synthetic substances that pose a high risk to human health and the environment. These substances have been found around the world, including some areas far from those where these pollutants were used, such as polar areas, as well as in human populations and even in breast milk. To address this problem at a global level, the Stockholm Convention was signed on May 23, 2001. The text of the convention describes the properties of POPs as follows: “Persistent organic pollutants have toxic properties, are persistent to degradation, bioaccumulate and are transported by air, water and migratory species, across international borders and deposited far from the place of their release, accumulating in terrestrial and aquatic ecosystems” (García, Olaya, & Sierra, 2017).

Turmeric

It is a herbaceous plant of the Zingiberaceae family originating from Southeast Asia, commonly known for its medicinal properties in traditional Indian medicine. This plant is used as a food flavoring, has cosmetic properties, and has also been used in the protection and treatment of skin, liver, and digestive conditions and against intestinal parasites, as a remedy for poisons and snake bites (García, Olaya, & Sierra, 2017).

Turmeric rhizome has been the subject of much research, attempts have been made to find its active principles in order to optimize its activity and explain its mechanism of action; numerous extracts have been prepared, ethanolic, methanolic and with different solvents to analyze its biological activities. (García, Olaya, & Sierra, 2017).

Turmeric rhizome has been the subject of much research, attempts have been made to find its active principles in order to optimize its activity and explain its mechanism of action; numerous extracts have been prepared, ethanolic, methanolic and with different solvents to analyze its biological activities (Saiz-de-Cos, 2014).

Both the EFSA (European Food Safety Authority) and the OCU (Consumers and Users Organization) advise against taking it as a medicine, unless it is prescribed by a doctor, and the latter organization warns that it has not been ruled out that turmeric was the cause of several cases of hepatitis that were discovered in 2019 in Italy and Belgium. They also warn that it can be dangerous to take more than the recommended 210 mg per day for an adult weighing around 70 kg, whether it is found in food products, infusions or pills (Segura, 2021).

However, if it is taken only as a spice or in an infusion, which is very fashionable, its effects may not be noticeable, since curcumin only represents five percent of the total weight of turmeric, insufficient to have an influence on health. In addition, since it is not water-soluble, it is difficult to absorb into the bloodstream and enormous quantities of the turmeric spice would be needed to notice its effects. It has not been ruled out that taking turmeric contributes to making many people feel better, but it is known that it can cause health problems if not done under proper medical supervision (Segura, 2021).

Despite its widespread consumption and uses, turmeric has not been thoroughly screened for adulteration, but it has been identified as a source of Pb exposure in South Asia and is a threat to public health as even low levels of exposure can reduce IQ and disrupt normal cognitive development, especially among children. A study in rural Munshiganj district of Bangladesh found that 78% of 309 children aged 20–40 months had elevated blood lead levels, and that turmeric was the likely route of exposure. The study found that lead chromate (PbCrO₄), a yellow pigment, was added to dried turmeric for the purpose of enhancing its shine (Forsyth, J.E.; Nurunnahar, S.; Islam, S.S.; Baker, M.; Yeasmin, D.; Islam, M.S.; Rahman, M.; Fendorf, S.; Ardoin, N.M.; Winch, P.J.; Luby, S.P., 2019).

Curcumin prevents the proper absorption of iron. There is no evidence that its consumption is free of adverse effects in children under 18 years of age. This substance and its metabolites are transferred to babies through breast milk. It has not been possible to identify how supplements containing curcumin would affect pregnancy and breastfeeding (Lorinczova H. T., Begum G., Renshaw D. and Zariwala M. G., 2021)

Pollutants degradation

Concept

Environmental pollution is defined as the presence in the environment of any agent (physical, chemical or biological) or a combination of several agents in places, forms and concentrations such that they may be harmful to the health, safety or well-being of the population, to plant or animal life, or prevent the normal use of the properties of a given area (Arbeli, 2009).

Classification

One of the most common classifications is based on their operating principles, such as biological, physicochemical and thermal (Cabrerá, 2015).

- Retention: confinement in cells, impermeable barriers, fixation, etc.
- Extraction or separation: filtration by activated carbon, washing with surfactants, extraction of free product, extraction of vapors, etc.
- Destruction: bio-restoration, Phyto-restoration, incineration, etc. Another classification is based on the effect on the pollutants produced by the sanitation techniques. In this way, there are retention, extraction, separation and destruction techniques (Cabrera, 2015).

In practice, the two classifications mentioned are valid and even complementary.

Remediation strategies

There are three basic strategies that can be used separately or together to remediate most contaminated sites (Volke-Sepúlveda & Velasco-Trejo, 2002) :

- Destruction or modification of contaminants: This type of technology seeks to alter the chemical structure of the contaminant.
- Extraction or separation: Contaminants are extracted and/or separated from the contaminated medium, taking advantage of their physical or chemical properties (volatilization, solubility, electrical charge).
- Isolation or immobilization of the contaminant: Contaminants are stabilized, solidified or contained using physical or chemical methods.

1.6 ZrO₂ as a photocatalysts, State-of-the art.

Botta et al. (Botta, Navío, Hidalgo, & Gloria M. Restrepo, 1999) studied the photocatalytic properties of sol-gel prepared ZrO₂ and Fe/ZrO₂ semiconductors, which were used in heterogeneous catalysis, Zr was considered as a photochemical photocatalyst for heterogeneous reactions. Comparative tests were performed between ZrO₂ and TiO₂; the photocatalytic efficiency of pure ZrO₂ and with Fe content of 0.5-20 % was tested in nitrite, EDTA and Cr (VI) and compared with TiO₂, all samples were active, although the efficiency was lower than that of TiO₂.

Uganbayar et al. (Uganbayar, Wen, Mostafa, & Bilge, 2014) reported in their work “Effect of Niobium on the Defect Chemistry and Oxidation Kinetics of Tetragonal ZrO₂” that they used density functional theory calculations to predict the effect of Nb on defect equilibria in the tetragonal phase of ZrO₂, they discuss how changes in defect concentration affect the protection of this natively grown oxide in Zr alloys during oxidation. This was done with the purpose of determining the mechanisms by which Nb affects the corrosion and strength of zirconium alloys in nuclear reactor application.

In present work, the obtaining of ZrO₂ is proposed, using sol-gel method in a basic medium. The material obtained was characterized by Raman Spectroscopy, X-Ray Diffraction (XRD), Scanning Electron Microscopy (SEM) and Energy Dispersive Spectroscopy (ED) to determine present phases, crystalline lattice, surface morphology and elemental composition, respectively.

Experimental setup

Sol-gel synthesis

To obtain ZrO₂, distilled H₂O was mixed with ammonia (Mercury, 26°), stirred magnetically for 5 minutes at room temperature; Subsequently, isopropyl alcohol (La Moderna, R.A purity) was added, it was kept stirring for 1 min, then Zirconium (IV) propoxide (Sigma-Aldrich, 70%W in propanol) was placed, the solution was kept for one hour. in stirring at room temperature, for the formation of the sol. Different molar proportions of precursor were used for the synthesis of the material, for M1 and M2 are NH₃ 20 mol, Isopropyl alcohol 8mol and Zirconium (IV) Propoxide 1 mol, respectively. For M3 and M4 are NH₃ 10 mol, Isopropyl alcohol 8 mol and Zirconium (IV) Propoxide 1 mol, respectively.

The Sol was aged for 24 h at room temperature to obtain a gel. Subsequently, it was placed in a drying oven to evaporate the remnants of the synthesis at 70 °C for 24 h. After drying, a white amorphous powder is obtained.

2.2 Thermal Treatment (TT)

To determine the formation temperatures of ZrO_2 phases, a Linkam hot cell coupled to the μRaman equipment was used. 0.1 g of ZrO_2 was placed on a silicon wafer; heating ramps with different temperatures were programmed at different times. It started at 450 °C, followed by 50 °C until reaching 600 °C, holding the temperature for 2 h, with a heating rate of 30 °C/min. Subsequently, a second ramp programming was done with temperatures of 1000 °C and 1200 °C, with a time of 2 h each. At the end of time at each temperature, the material was analyzed in μRaman , to correlate the structural behavior of the material as a function of temperature; It also served to determine the ideal temperature to reach the desired phase. After determining the conditions to obtain each phases, the samples were subjected to heat treatment, for M1 at 1200°C and 2 h, for M2 at 450°C and 3 h, for M3 at 800°C and 5 h and M4 at 600 °C and 6 h. The intention of annealing was to obtain the tetragonal phase of the material, since it is the best for the photocatalysis process (Rani, y otros, 2022).

Turmeric solution

A stock solution of turmeric was prepared at a concentration of 0.1 mol/L, with 500 mL of distilled water at a temperature of 50 °C for a time of 90 min until the dye was completely dissolved. The solution was then allowed to cool, to be stored and labeled.

Material Characterization

It is important to highlight that all the samples prepared in this work were characterized before and after thermal treatment, to have the complete history of the material.

2.4.1 Scanning Electron Microscopy (SEM) and Energy Dispersive Spectroscopy (EDS)

The morphology and elemental chemical composition of the samples were obtained with the help of a JEOL JSM-IT100 SEM coupled to an X-ray microprobe for elemental analysis (ED); secondary and backscattered electron signals were used in high vacuum mode. A voltage of 20KV at 500, 1000 and 1500x magnification, were used.

2.4.2 μRaman Spectroscopy.

The crystalline structure of ZrO_2 was analyzed by μRaman spectroscopy, using a Horiba Yvon Jovin μRaman equipment model XploraPlus. Raman scattering was induced using a solid-state laser ($\lambda=532$ nm, 25mW maximum power), with a 10% neutral optical density filter. The beam is focused on the sample with a 50x objective and this same is used to collect the scattered light; a 1200 l/mm grating was used, 50 acquisitions of 3 s exposure each were averaged.

2.4.3 X-Ray Diffraction.

The identification of crystalline phases and lattices were carried out using a Bruker D8 Discovery Diffractometer for powders with a Cu source ($\lambda= 1.54 \text{ \AA}$), in 2 θ mode from 10° to 66°. A step of 0.01°, acquisition time of 1 s, a voltage of 40 KV and a current of 30 mA were used.

2.4.4 UV-Vis Spectroscopy

The photocatalytic performance of the material was evaluated using a Thermo Scientific Evolution 220 UV-Vis spectrophotometer in absorbance mode. Spectra were recorded in a range of 190 to 800 nm, with a scanning speed of 480 nm/min and a resolution of 1 nm.

2.5 Photocatalytic Experiment.

The photocatalytic experiment was carried out using a UV light lamp placed on the top of a container designed with the intention of isolating the interaction of the material with ambient light, a heated magnetic stirrer was introduced, with 50 mL of turmeric solution in a beaker, at a working distance of 6.9 cm between the light and the surface of the solution.

The solution was stirred for 10 min to homogenize it, then 0.024 g of ZrO₂ was added and stirring was continued for additional 10 min; the solution was allowed to stand for 5 min and the initial absorbance was measured with the help of a UV-Vis Spectrophotometer. An aliquot of 3 mL was taken from the solution every 10 min and its absorbance was measured for a total time of 2 h.

The formula 1 for percent degradation (% Deg) described by Susmita (Paul & Choudhury, 2014), was employed to study the removal of natural dye turmeric.

$$\%D: \frac{A_0 - A_t}{A_0} * 100$$

[1]

Where: A₀: initial absorbance, A_t: absorbance after a time t.

Results Analysis

The results are divided into two parts, the first analyzes the synthesis and characterization of the material and the second the photocatalytic tests.

Raman Spectroscopy

Sample without TT

The as-synthesized material was characterized with μRaman spectroscopy to determine the crystalline structure of the material. In Figure 4, there are no characteristic signals of crystalline phases; the material is amorphous. In all the samples prepared, the same behavior was observed.

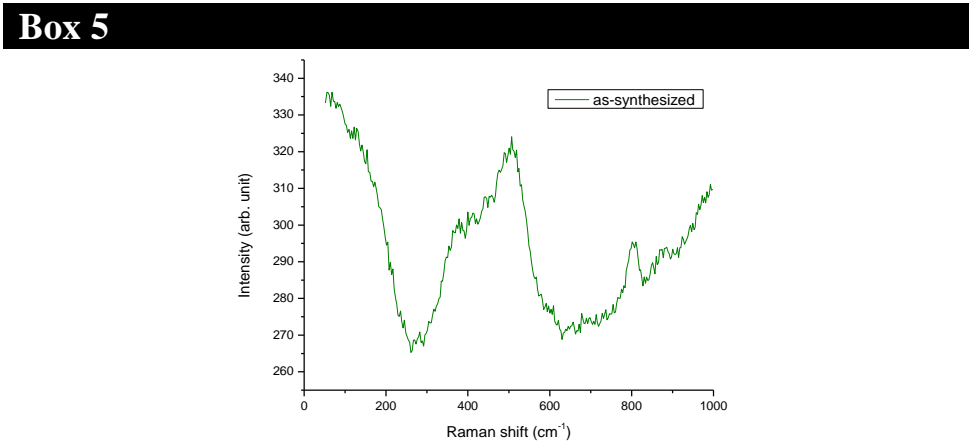


Figure 4
Raman spectrum for as-synthesized sample.

Source: Own elaboration

Samples with TT

The Raman spectrum of sample M1, which was obtained at a temperature of 1200 °C and a time of 2 h (Figure 5a)), showed signals are in good agreement with taha reported the literature (Kurpaska, y otros, 2016) and that correspond to the monoclinic phase of ZrO₂, the vibrational modes are located in the positions: 180, 188, 221, 380, 476, 608 y 640 cm⁻¹. In the case of sample M2, according to what was reported by Sohn et al. (Sohn, Chun, & Pae), the peaks that correspond to the tetragonal phase are found with the following shift values: 148, 263, 325, 406, 472, 608 and 635 cm⁻¹, as shown in Figure 5 b). Although a small contribution from the monoclinic phase (M) was also found.

In the spectrum of figure 5 c), the different peaks of the signals that correspond to sample M3 are shown. According to the author D. Thackeray (Thackeray, 1974), the signals found in the Raman spectrum correspond to the cubic phase and They are located at positions: 147, 259, 317, 456 and 606 cm⁻¹, although some small signals were found that correspond with the monoclinic phase (M). Analyzing the Raman spectrum obtained for sample M4 (Figure 5 d)) it can be observed that there is a mixture of phases and according to the authors cited previously (Sohn, Chun, & Pae) (Kurpaska, y otros, 2016) (Thackeray, 1974) They belong to the tetragonal and monoclinic phases.

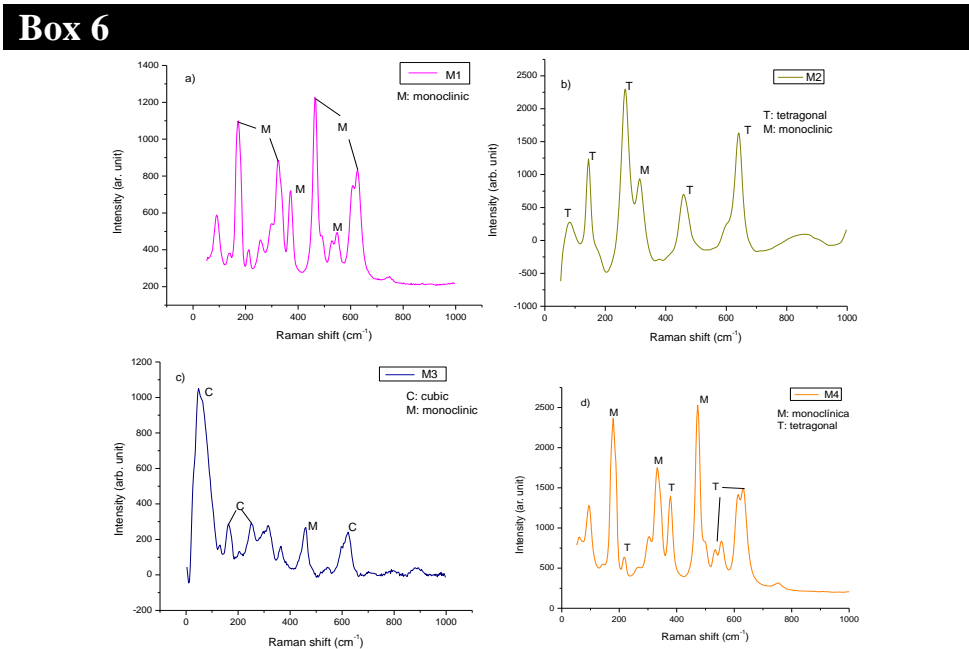


Figure 5
Raman spectrum for a) Sample M1, monoclinic phase, b) Sample M2, tetragonal phase, c) Sample M3, cubic phase and d) Sample 4, mixture of phase.

Source: Own elaboration

3.2 X-Ray Diffraction (XRD)

Figure 6 from a) to d), shows the diffractograms of the samples obtained after the thermal treatment of ZrO_2 . The 2θ angular range explored is 10 to 66° , with a step of 0.01° and an acquisition time of 1 s per point that allows adequate resolution of the peaks.

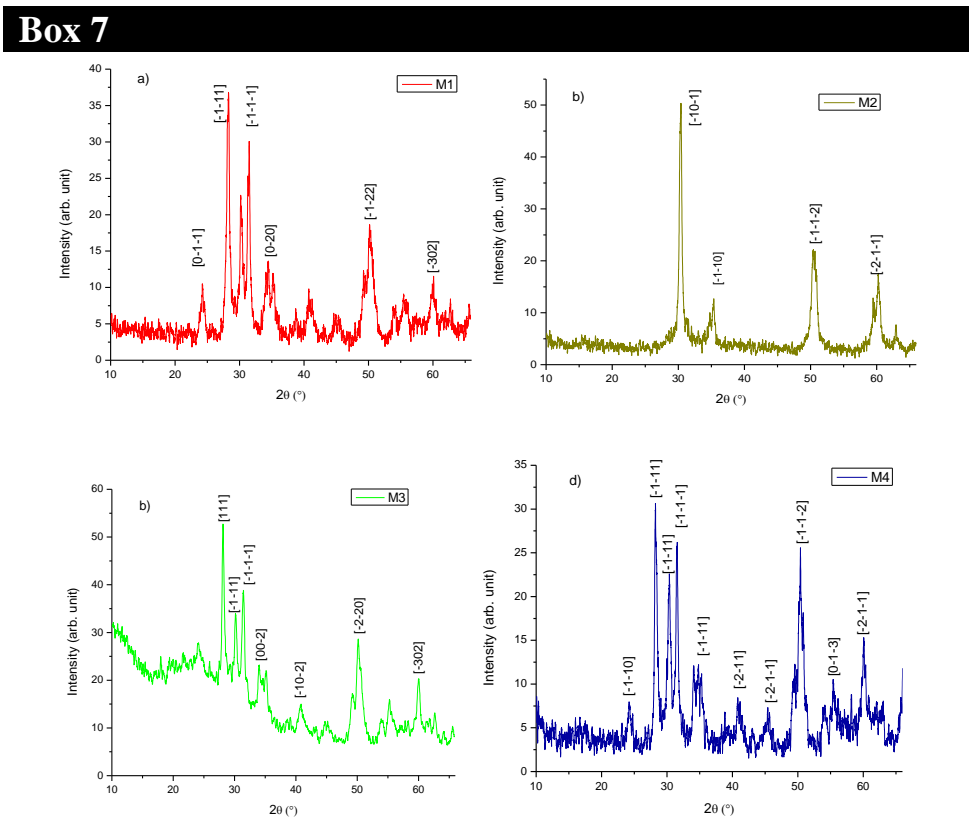


Figure 6
X-Ray spectra a) M1: monoclinic phase, b) M2: tetragonal phase, c) M3: cubic phase, d) M4: mixture of phase.

Source: Own elaboration

The positions of the diffraction peaks presented were identified using the DIFRACT.EVA program and they coincide with COD 9007485 (cubic phase), COD 1522143 (monoclinic phase) and COD 1525706 (tetragonal phase) card; with this information all spectra were indexed to know the preferential direction in each sample.

3.3 Scanning Electron Microscopy.

In figure 7, micrographs of sample M1 are observed. In figure 7a, M1 does not have a thermal treatment (TT), it has a porous and shapeless morphology; when a TT is applied (see figure 7b) the powder begins to agglomerate. The micrographs of sample M2 are shown in figure 7c and 7d. In figure 7c, we can see a porous morphology in the shape of small spheres, while in figure 7d it can be seen as the powder becomes flat and compact. In sample M3, when a TT is not applied to the material, it does not have a defined morphology (Figure 7e), with the formation of small grains; however, when the treatment is applied, it can be appreciated how the material begins to become lumpy (figure 7f). Figure 7g shows the micrographs corresponding to sample M4. Without TT, the morphology presents a tendency towards the formation of facets with porosity; while in Figure 7h, there is a dispersion of these facets to form small lumps without a specific shape.

Box 8

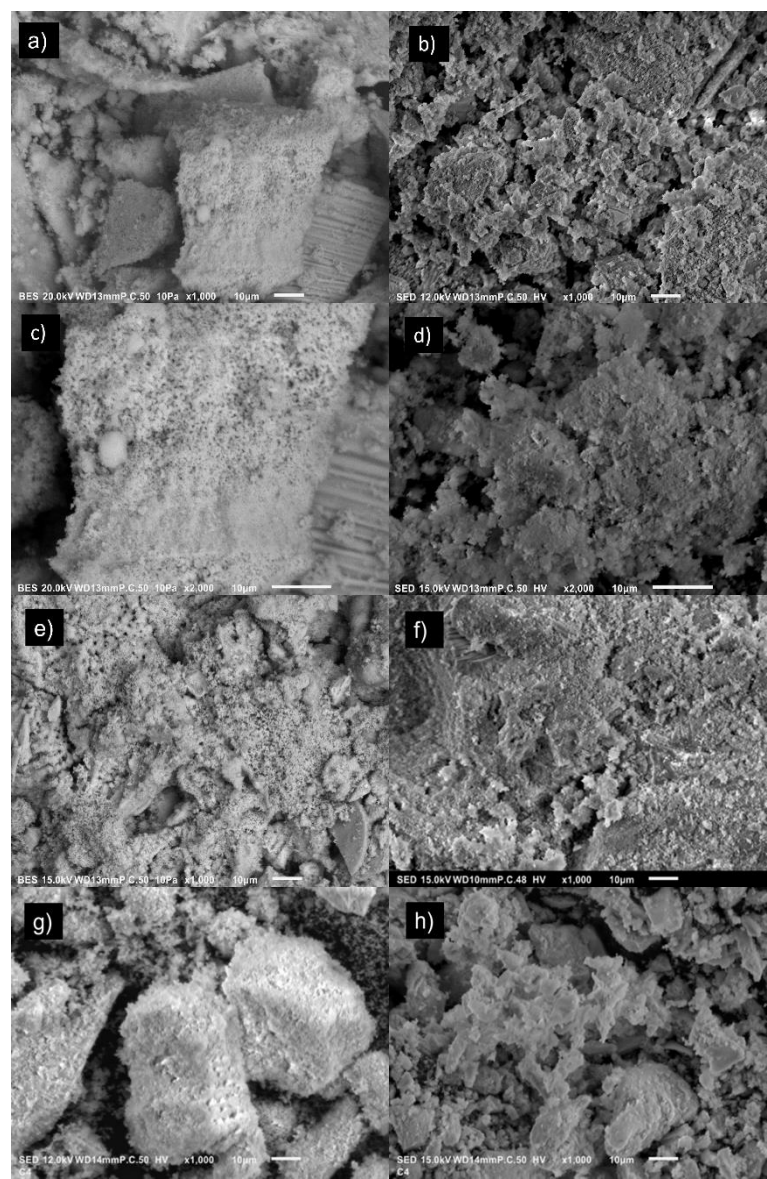


Figure 7
Micrographs of samples M1; a) without TT, b) with TT., sample M2; c) without TT, d) with TT., sample M3; e) without TT, f) with TT and sample M4; g) without TT, h) with TT.

Source: Own elaboration

Elemental composition (EDS)

To determine elemental composition, Energy Dispersive Spectroscopy was carried out to all samples, the elemental analysis was carried out on all the samples. A single analysis is shown because the compositions of the four samples are the same. The elemental analysis for sample M1 shows Carbon (5.84 %W), Oxygen (28.46 %W) and Zirconium (63.95 %W), the elements that make up ZrO_2 were found, and it is possible to see that there is no presence of contaminants.

Photocatalytic activity

The photocatalytic activity of ZrO_2 from sample M1 to M4 was evaluated with the photodegradation of the natural dye turmeric using UV light. The results showed (Figure 8) that the monoclinic and cubic phases do not present degradation; while the tetragonal phase degrades 24.98% and the mixture of phases (tetragonal and monoclinic) degrades turmeric by 14.07%.

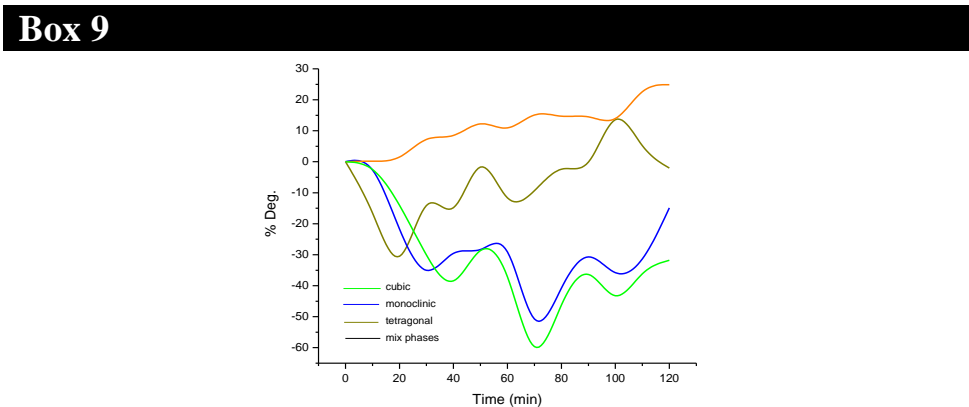


Figure 8
Photocatalytic activity of all simples.

Source: Own elaboration

Conclusion

ZrO_2 was synthesized by sol-gel, ammonia was used as a catalyst, different phases were found such as: monoclinic, tetragonal, cubic and a mixture of tetragonal with monoclinic; for different thermal treatment temperatures; so, the conditions for obtaining each of them could be determined. The phases present in the material were verified using Raman analysis and X-ray Diffraction techniques. The elemental composition and morphology were studied using Scanning Electron Microscopy, with which the presence of Zr and O in all samples was exclusively verified.

The behavior of the 4 samples obtained from ZrO_2 as a photocatalyst was evaluated. The phases that can degrade the organic pollutant turmeric are the tetragonal one with 24.98% degradation and the mixture of phases (tetragonal and monoclinic) with 14.07% degradation. be the best samples for the degradation process, while the monoclinic and cubic phases do not present degradation. The constant stirring of the photocatalyst with the turmeric solution is decisive in this process, since it helps to achieve a better balance in the dispersion of the photocatalyst in the aqueous medium and causes the UV light to excite the ZrO_2 and photocatalysis occurs.

Declarations

Conflict of interest

The authors declare no interest conflict. They have no known competing financial interests or personal relationships that could have appeared to influence the article reported in this article.

Author contribution

Sánchez-Montiel, Dulce D.: Contributed to the synthesis of the materials studied in the article.

Castrejón-Sánchez, Victor Hugo: Contributed to the project idea, the characterization, and the discussion of the results of the materials studied in the article.

Enríquez-Pérez, Ma. Angeles: Contributed to the project idea, the characterization, and the discussion of the results of the materials studied in the article.

García-González, Nidia: Contributed to the project idea, the characterization, and the discussion of the results of the materials studied in the article.

Availability of data and materials

The synthesized materials and all the data from the analyses carried out in this research are available.

Funding

We thank TecNM for the financial support through “Convocatoria 2024 Proyectos de Investigación Científica, Desarrollo Tecnológico e Innovación”.

Acknowledgements

The authors thank the Academy-Industry Cooperation Center of the Tecnológico de Estudios Superiores de Jocotitlán for all the support provided through access to the XRD, Raman, SEM and EDS equipment.

Abbreviations

XRD	X-ray diffraction
EDS	Energy Dispersive Spectroscopy
SEM	Scanning Electron Microscopy.
ZrO ₂	Zirconium Dioxide

References

Antecedents

Andrade-Guel, M. L., Cabello-Alvarado, C. J., & Ávila-Orta, C. A. (2019). [Dióxido de zirconio: alternativas de síntesis y aplicaciones biomédicas](#). *Biología y Química*, 14(1), 18-30. ISSN 2007-7521.

Arbeli, Z. (2009). [Biodegradation of persistent organic pollutants \(POPs\): I the case of polychlorinated biphenyls \(PCB\)](#). *Acta biol. Colomb.*, 14(1), 57-88.

Bashir, S., & Louise, J. (2015). [Advanced nanomaterials and their applications in renewable energy](#). Netherlands: Elsevier. ISBN:978-0-12-801528-5,

Beatriz. (2011, mayo 26). [Dióxido de circonio](#). Retrieved septiembre 29, 2024.

Botta, S. G., Navío, J. A., Hidalgo, M. C., & Gloria M. Restrepo, M. a. (1999). [Photocatalytic properties of ZrO₂ and Fe/ZrO₂ semiconductors prepared by a sol–gel technique](#). *Journal of Photochemistry and Photobiology A: Chemistry*, 129(1-2), 89-99.

Cabrera, L. M. (2015). [Técnicas biológicas para la degradación de contaminantes](#). Tesis de licenciatura en Ciencias Biológicas. Quito: Pontificia Universidad Católica de Ecuador.

Candal, R. J., Bilmes, S. A., Blesa M. A., (n.d.). [SEMICONDUCTORES CON ACTIVIDAD FOTOCATALÍTICA](#). Universidad de Córdoba Colombia.

- Carballo-S., L. M., & Galindo-V., H. M. (2001). Estudio de los Procesos Sol-gel para la Obtención de un Aglutinante Apropriado para el Peletizado de Alúmina. *Revista Ingeniería e Investigación*, 48:57-63.
- Castrejón-Sánchez, V., Enríquez-Pérez, M. Á., Rosales-Davalos, J., & Díaz-Camacho., F. J. (2018). Síntesis y caracterización de materiales nanoestructurados de TiO₂ por el método sol gel. *Revista de Energía Química y Física*, 5(16), 37-43. ISSN: 2410-3934
- Cubillos, I., Olaya, J. J., Bethencourt, M., Cifredo, G. & Marco, J. F., (2012). Producción y caracterización de películas de óxido de circonio por spray pirólisis. *Revista Latinoamericana De Metalurgia Y Materiales*, 33(1), 116-130. ISSN 0255-6952.
- Deshmane, V. G., & Adewuyi, Y. G. (2012). Synthesis of thermally stable, high surface area, nanocrystalline mesoporous tetragonal zirconium dioxide (ZrO₂): Effects of different process parameters. *Mesoporous Material*, 148(1), 88-100.
- Ecológicos, M. (2024, 09 10). *Materiales Ecológicos*.
- Forsyth, J.E., Nurunnahar, S., Islam, S.S., Baker, M., Yeasmin, D., Islam, M.S., Rahman M., Fendorf S., Ardoin N. M., Winch P. J., Luby, S. P. (2019). Turmeric means "yellow" in Bengali: Lead chromate pigments added to turmeric threaten public health across Bangladesh. *Environmental Research*, 179, 108722. ISSN 0013-9351,
- Fujishima, A., Zhang, X., & Tyrk, D. A. (2008). TiO₂ photocatalysis and related surface phenomena. *Surface Science Reports*, 515-582. ISSN 0167-5729.
- García ALL, Olaya MQJH, Sierra AJI, Padilla SL. (2017). Actividad biológica de tres Curcuminoides de *Cúrcuma longa* L. (Cúrcuma) cultivada en el Quindío-Colombia. *Rev Cubana Plant Med.*, 22(1), 1-14. ISSN 1028-4796.
- Gutiérrez, M., & Castellanos, M. (2021). Síntesis por el método sol-gel aplicado al estudio del polimorfismo en nanopartículas de TiO₂. *Mundo nano. Revista interdisciplinaria en nanociencias y nanotecnología*, 4(1), 67-73.
- Lisbona-García, L. E. (2016). *MATERIALES FOTOCATALÍTICOS Y SUS APLICACIONES EN CONSTRUCCIÓN*. Cataluña: Universitat Politècnica de Catalunya.
- LODEPA. (2023). *Revisión bibliográfica: Problemática de calidad de aire interior en el puesto de trabajo y ambiente hospitalario*. Comparativa entre métodos de descontaminación de aires. Madrid: LODEPA.
- López, V. (2015, 02 13). *La fotocatalisis*. Interempresas.
- Lorinczova H. T., Begum G., Renshaw D. and Zariwala M. G. (2021). Acute Administration of Bioavailable Curcumin Alongside Ferrous Sulphate Supplements Does Not Impair Iron Absorption in Healthy Adults in a Randomised Trial. *Nutrients*, 13(7), 2300.
- Mosquera, E., Rosas N., Debut, A. & Guerrero, V.H. (2015). Síntesis y Caracterización de Nanopartículas de Dióxido de Titanio Obtenidas por el Método de Sol-Gel. *Revista Politécnica*, 36(3), 1-7. ISSN-e 2477-8990
- Nevárez-Martínez, M. C., Espinoza-Montero, P. J., Quiroz-Chávez, F. J., & Ohtani, B. (2017). Fotocatalisis: inicio, actualidad y perspectivas a través del TiO₂. *Avances en Química*, 12(2-3), 45-59.
- Ochoa, Y., Ortigón, Y., & Rodríguez Páez, J. E. (2010). Síntesis de TiO₂, fase anatasa, por el método sol-gel: estudio del efecto de la presencia de AcacH en el sistema. *Revista Facultad de Ingeniería Universidad de Antioquía*, 52, 29-40. ISSN 0120-6230 On-line, ISSN 2422-2844
- Otgonbaatar, U., Ma W. Youssef M., Yildiz B. (2014). Effect of Niobium on the Defect Chemistry and Oxidation Kinetics of Tetragonal ZrO₂. *The journal of Physical Chemistry*, 118(35), 20122-20131.

Pierre, A. C. (1998). [Introduction to sol-gel processing](#). New York: Springer.

Ramírez-Riaño, D. A. (2017). [Síntesis por Sol-Gel de un recubrimiento Nanoestructurados de TiO₂ para ser aplicado en sustrato de vidrio](#). Bogotá: Universidad de Bogota Jorge Tadeo Lozano.

Saiz-de-Cos, P. (2014). [Cúrcuma I \(*Curcuma longa* L.\)](#). Reduca(Biología) Serie Botánica, 7(2), 84-99. ISSN: 1989-3620.

Sánchez, D., Esteban, H., Ceja, A., & Altilano, F. (2017)31-36). [Preparación de SiO₂ por los métodos no hidrotérmico y Sol-Gel para adsorción de colorantes](#). Revista de Energía Química y Física, 4(13).

Segura, A. (2021, 05 12). [Los riesgos de abusar de la cúrcuma](#). La Vanguardia.

Vagkopoulou, T., Koutayas. S.O., Koidis, P., Jörg Rudolf Strub J.S. (2009). [Zirconia en odontología: primera parte. Descubriendo la naturaleza de una nueva biocerámica](#). The European Journal of Esthetic Dentistry, 2(4), 274-295.

Volke-Sepúlveda, T., & Velasco-Trejo, J. a. (2002). [Tecnologías de remediación para suelos contaminados](#). México: Instituto Nacional de Ecología-SEMARNAT. ISBN: 968-817-557-9

Zarazúa-Acosta, A. (2023). [OBTENCIÓN Y CARACTERIZACIÓN DE MEZCLAS DE POLVOS DE Bi₂O₃ Y TiO₂ PARA APLICACIONES FOTOCATALÍTICAS](#). Querétaro: Universidad Autónoma de Querétaro.

Basics

Rani, V., Sharma, A., Abhinandan K., Singh, P., Thakur, S., Singh, A., Le Q. V., Nguyen V. H., Raizada, P. (2022). [ZrO₂-Based Photocatalysts for Wastewater Treatment: From Novel Modification Strategies to Mechanistic Insights](#). Catalysts, 12, 1418-1436.

Paul, S., & Choudhury, A. (2014). [Investigation of the optical property and photocatalytic activity of mixed phase nanocrystalline titania](#). Applied Nanoscience, 4, 839-847.

Supports

Kurpaska, L., Lesniak, M., Jadach, R., Sitarz, M., Jasinski, J., & Grosseau-Poussard, J.-L. (2016). [Shift in low-frequency vibrational spectra measured in-situ at 600 °C by Raman spectroscopy of zirconia developed on pure zirconium and Zr-1%Nb alloy](#). Journal of Molecular Structure, 1126, 186-191.

Sohn, J. R., Chun, E. W., & Pae, Y. I. (2003). [Spectroscopic Studies on ZrO₂ Modified with MoO₃ and Activity for Acid Catalysis](#). Bulletin of the Korean Chemical Society, 24 (12). pISSN:0253-2964/ eISSN:1229-5949

Thackeray, D. (1974). [The Raman spectrum of zirconium dioxide](#). Spectrochimica Acta part A, 30 (12), 549-550.

Discussions

Kurpaska, L., Lesniak, M., Jadach, R., Sitarz, M., Jasinski, J., & Grosseau-Poussard, J.-L. (2016). [Shift in low-frequency vibrational spectra measured in-situ at 600 °C by Raman spectroscopy of zirconia developed on pure zirconium and Zr-1%Nb alloy](#). Journal of Molecular Structure, 1126, 186-191.

Sohn, J. R., Chun, E. W., & Pae, Y. I. (2003). [Spectroscopic Studies on ZrO₂ Modified with MoO₃ and Activity for Acid Catalysis](#). Bulletin of the Korean Chemical Society, 24 (12). pISSN:0253-2964/ eISSN:1229-5949

Thackeray, D. (1974). [The Raman spectrum of zirconium dioxide](#). Spectrochimica Acta part A, 30 (12), 549-550.